Hydrolysis of β-Lactam Antibiotics Catalyzed by Dinuclear Zinc(II) Complexes: Functional Mimics of Metallo-β-lactamases

Natalia V. Kaminskaia, Bernhard Spingler, and Stephen J. Lippard*

Contribution from the Department of Chemistry, Massachusetts Institute of Technology, Cambridge, Massachusetts 02139

Received October 15, 1999. Revised Manuscript Received February 15, 2000

Abstract: Three stable dinuclear zinc(II) complexes, $[Zn_2L_1(\mu\text{-}NO_3)(NO_3)_2]$ and $[Zn_2L_1(\mu\text{-}OMe)(NO_3)_2]$, where L_1 is 2,6-bis{[*N*-(2-dimethylaminoethyl)-*N*-methyl]aminomethyl}-4-methylphenolate, and $[Zn_2L_2(NO_3)_3]$, where L_2 is 2-{[*N*-(2-dimethylaminoethyl)-*N*-methyl]aminomethyl}-4-bromo-6-{[*N*′-2-(2′-pyridyl)ethyl]aminomethyl}-phenolate, were synthesized and characterized in the solid state and in aqueous solution. These complexes catalyze the hydrolysis of penicillin G and nitrocefin, serving as functional synthetic analogues of the metallo-β-lactamases, bacterial enzymes responsible for antibiotic resistance. The mechanism of the hydrolysis was studied in detail for the catalyst precursor $[Zn_2L_1(\mu\text{-}NO_3)(NO_3)_2]$, which converts into $[Zn_2L_1(\mu\text{-}OH)(NO_3)_n(sol)_{2-n}]^{(2-n)+}$ in the presence of water. The complex $[Zn_2L_1(\mu\text{-}OH)(NO_3)_2]$ ($n = 2$) was characterized in the solid state. Initial coordination of the substrate carboxylate group is followed by the rate-limiting nucleophilic attack of the bridging hydroxide at the β-lactam carbonyl group in aqueous solution. The product is formed upon fast protonation of the intermediate. Mononuclear complexes Zn(cyclen)$(NO_3)_2$ and Zn(bpta)$(NO_3)_2$ are as reactive in the β-lactam hydrolysis as the dinuclear complexes. Consequently, the second zinc ion is not required for catalytic activity.

Introduction

Approximately half of the commercially available antibiotics are β-lactams.[1] In recent years, bacterial resistance to a wide range of antibiotics has become so prevalent that some infections can no longer be successfully treated.[1−3] A common reason for resistance to β-lactam antibiotics in bacteria is their ability to express β-lactamases, enzymes that catalyze the hydrolytic opening of the β-lactam ring, as depicted in eq 1 for the

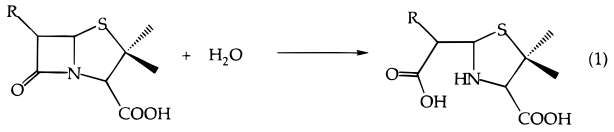

(1)

penicillin derivatives. Unlike the parent β-lactam, the hydrolysis product does not interfere with cell wall biosynthesis and is therefore harmless to bacteria. The high periplasmic concentrations of β-lactamases, in addition to their efficiency, ensure that β-lactam antibiotic drugs are hydrolyzed before reaching their targets.[4]

Among the more than 200 β-lactamases that have been identified to date[5] the majority (>90%) share an active-site serine residue and are collectively termed serine β-lactamases. Their well-studied mechanism involves nucleophilic attack of the serine hydroxyl group at the β-lactam carbonyl group, followed by hydrolysis of the acyl-enzyme intermediate.[6] In contrast, the less abundant class B β-lactamases require divalent metal ions for catalytic activity.[6,7] Since only 18 of the many characterized β-lactamases are metallo-β-lactamases, the clinical threat imposed by these enzymes was initially underestimated.[8,9] Metallo-β-lactamases can hydrolyze a wide range of substrates, however, including cephamycins and imipenem, compounds resistant to the serine β-lactamases.[10,11] Moreover, the metallo-enzymes show little or no susceptibility to traditional β-lactamase inhibitors, such as clavulanic acid or sulbactam. Although there have been reports of molecules that inhibit metallo-β-lactamases, at present there are no clinically useful inhibitors.[12,13] Thus, the application of most available antibiotics has been severely compromised in bacteria that produce metallo-β-lactamases.

Most metallo-β-lactamases are monomers containing a single polypeptide chain composed of 220−230 residues.[6] Crystal structures are available for several enzymes in this class, from *Bacteroides fragilis*, *Bacillus cereus* II, and most recently from *Stenotrophomonas maltophilia*.[14−17] Whereas the sequences of

(1) Neu, H. C. In *The Chemistry of β-Lactams*; Page, M. I., Ed.; Blackie: Glasgow, 1992; pp 101−128.
(2) Massova, I.; Mobashery, S. *Acc. Chem. Res.* **1997**, *30*, 162−168.
(3) Cohen, M. L. *Science* **1992**, *257*, 1050−1055.
(4) Hechler, U.; Van Den Weghe, M.; Martin, H. H.; Frère, J.-M. *J. Gen. Microbiol.* **1989**, *135*, 1275−1290.
(5) Bush, K.; Jacoby, G. A.; Medeiros, A. A. *Antimicrob. Agents Chemother.* **1995**, *39*, 1211−1233.
(6) Page, M. I.; Laws, A. P. *Chem. Commun.* **1998**, 1609−1617.
(7) Davies, R. B.; Abraham, E. P. *Biochem. J.* **1974**, *143*, 129−135.
(8) Rasmussen, B. A.; Bush, K. *Antimicrob. Agents Chemother.* **1997**, *41*, 223−232.
(9) Walsh, T. R.; Gamblin, S.; Emery, D. C.; MacGowan, A. P.; Bennett, P. M. *J. Antimicrob. Chemother.* **1996**, *37*, 423−431.
(10) Bush, K. *Clin. Infect. Diseases* **1998**, *27*, S48−S53.
(11) Livermore, D. M. *J. Antimicrob. Chemother. Suppl. D.* **1998**, *41*, 25−41.
(12) Hammond, G. G.; Huber, J. L.; Greenlee, M. L.; Laub, J. B.; Young, K.; Silver, L. L.; Balkovec, J.; Proyer, K. D.; Wu, J. K.; Leiting, B.; Pompliano, D. L.; Toney, J. H. *FEMS Microbiol. Lett.* **1999**, *179*, 289−296.
(13) Toney, J. H.; Fitzgerald, P. M. D.; Grover-Sharma, N.; Olson, S. H.; May, W. J.; Sundelof, J. G.; Vanderwall, D. E.; Cleary, K. A.; Grant, S. K.; Wu, J. K.; Kozarich, J. W.; Pompliano, D. L.; Hammond, G. G. *Chem. Biol.* **1998**, *5*, 185−196.
(14) Concha, N. O.; Rasmussen, B. A.; Bush, K.; Herzberg, O. *Structure* **1996**, *4*, 823−836.
(15) Ullah, J. H.; Walsh, T. R.; Taylor, I. A.; Emery, D. C.; Verma, C. S.; Gamblin, S. J.; Spencer, J. *J. Mol. Biol.* **1998**, *284*, 125−136.
(16) Fabiane, S. M.; Sohi, M. K.; Wan, T.; Payne, D. J.; Bateson, J. H.; Mitchell, T.; Sutton, B. J. *Biochemistry* **1998**, *37*, 12404−12411.
(17) Carfi, A.; Pares, S.; Duée, E.; Galleni, M.; Duez, C.; Frère, J.-M.; Dideberg, O. *EMBO J.* **1995**, *14*, 4914−4921.

10.1021/ja993704l CCC: $19.00
Published on Web 06/20/2000

Scheme 1

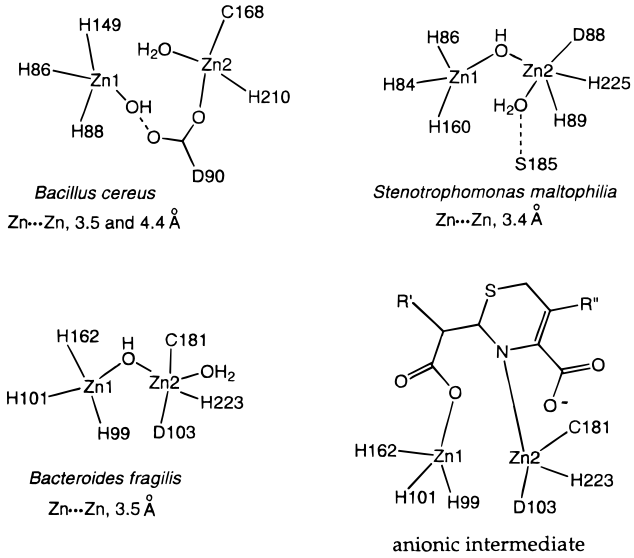

the first two enzymes are conserved (50 residues), the *S. maltophilia* enzyme has only 9 conserved amino acids. *B. fragilis* and *B. cereus* II β-lactamases have similar dizinc-binding motifs that include one cysteine, three histidine, and one aspartate residues. In the *S. maltophilia* β-lactamase, the cysteine residue is replaced by serine, resulting in the coordination of a second histidine to Zn(2). The structures are represented in Scheme 1.[10] The stability constants for the two zinc-binding sites differ, and β-lactamases have been isolated with only one zinc site occupied.[18,19] All three enzymes have a hydroxide ion that either bridges the two zinc(II) ions, as in the *S. maltophilia* and *B. fragilis* enzymes, or is coordinated to Zn(1) as in the *B. cereus* II β-lactamase. In the latter case, an aspartate carboxylate group serves to help link the two zinc(II) ions. The enzymes all have either lysine or serine residues at the active site. Hydrogen bonding between these residues and the conserved carboxylate group present in the antibiotics is proposed to position the substrate, although direct coordination of COO^- to the dizinc(II) center cannot be ruled out.[20]

The mechanism of action for class B β-lactamases has not been fully elucidated. By analogy with other metallohydrolases such as carboxypeptidase, catalysis is postulated to involve attack of a metal-bound hydroxide on the carbonyl group of the β-lactam ring followed by collapse of the tetrahedral intermediate.[14] Such a process seems inconsistent with the measured pH independence of k_{cat} and k_{cat}/K_m in the range 5.25−10.0,[21] however, since both attack by hydroxide ion and protonation of the departing nitrogen atom should be sensitive to pH. Perhaps the pK_a values are outside the measured range. More likely the pH independence of k_{cat} arises from the opposing pH effects on the nucleophilic attack and protonation, the two steps that contribute to k_{cat}. Recent reports suggest that cleavage of the amide bond occurs before protonation, with the resulting anionic intermediate being stabilized by coordination to zinc(II).[20,22] Protonation of this species is the rate-determining step. Site-directed-mutagenesis studies suggest that Asp-90, in

Scheme 2

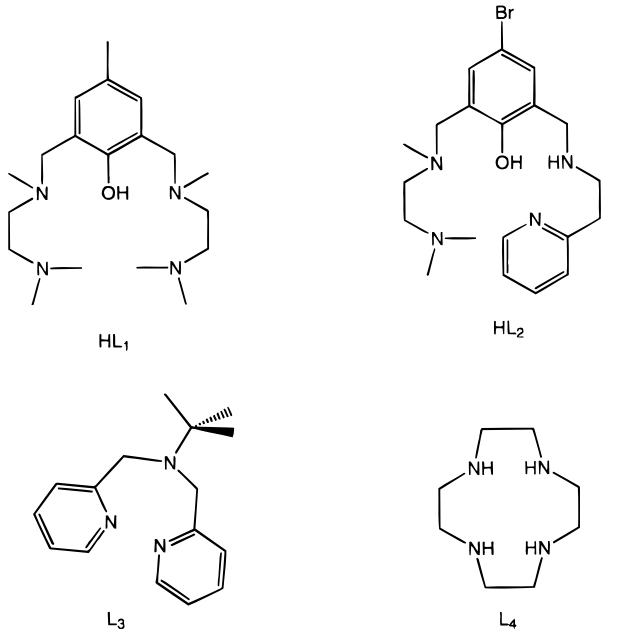

β-lactamase from *B. cereus*, may serve such a role as a general acid.[23] Despite this information, it is still uncertain whether hydrolysis occurs by general-base catalysis or whether zinc provides a local source of hydroxide ion. The possibility that the antibiotic carboxylate group may coordinate directly to zinc ions,[20] and the role of zinc bound in the second metal-binding site, have not been adequately addressed.

Because of the complexity of the enzyme, synthetic model compounds offer the potential to contribute mechanistic insights. Such information would both be of fundamental interest and could help in the design of mechanism-based inhibitors. With these objectives in mind, we have prepared three dinuclear zinc(II) complexes of ligands HL_1 and HL_2 (Scheme 2)[24] and have evaluated them as functional β-lactamase models for the hydrolysis of β-lactam antibiotics. The β-lactam hydrolytic reactivity of mononuclear analogues, formed by ligands L_3 and L_4, was also determined and compared to that of the dinuclear compounds.

Experimental Section

Chemicals. Deuterated compounds D_2O, DMSO-d_6, acetone-d_6, chloroform-d_1, and dichloromethane-d_2 were obtained from Cambridge Isotope Laboratories. Starting materials and reagents $Zn(NO_3)_2 \cdot 6H_2O$, $Zn(OTf)_2$, 2-(2-aminoethyl)pyridine, *N*,*N*,*N*′-trimethylethylenediamine, *p*-cresol, $NaBH_4$, 5-bromosalicylaldehyde, and cyclen were obtained from Aldrich. Succinic acid disodium salt hexahydrate, $LiOH \cdot H_2O$, and a 0.100 M standard solution of NaOH were obtained from Fluka. Alanine, penicillin G (sodium salt), and cephalothin (sodium salt) were obtained from Sigma. The hydrolytic substrate nitrocefin (2-(2,4-dinitrostyryl)-(6*R*,7*R*)-7-(2-thienylacetamide)-ceph-3-em-4-carboxylic acid, E isomer) was kindly donated by Merck. These and all other chemicals were of reagent grade.

Physical Measurements. ^1H and ^{13}C NMR spectra were obtained at 500 and 125 MHz, respectively, on Varian 500 and 501 NMR spectrometers. UV−visible spectra were recorded on a Cary 1E spectrophotometer equipped with a temperature-controlled unit. Solution

(18) Paul-Soto, R.; Hernandez-Valladares, M.; Galleni, M.; Bauer, R.; Zeppezauer, M.; Frère, J.-M.; Adolph, H.-W. *FEBS Lett.* **1998**, *438*, 137−140.

(19) Paul-Soto, R.; Bauer, R.; Frère, J.-M.; Galleni, M.; Meyer-Klaucke, W.; Nolting, H.; Rossolini, G. M.; de Seny, D.; Hernandez-Valladares, M.; Zeppezauer, M.; Adolph, H.-W. *J. Biol. Chem.* **1999**, *274*, 13242−13249.

(20) Wang, Z.; Fast, W.; Benkovic, S. J. *Biochemistry* **1999**, *38*, 10013−10023.

(21) Wang, Z.; Benkovic, S. J. *J. Biol. Chem.* **1998**, *273*, 22402−22408.

(22) Wang, Z.; Fast, W.; Benkovic, S. J. *J. Am. Chem. Soc.* **1998**, *120*, 10788−10789.

(23) Lim, H. M.; Iyer, R. K.; Pène, J. J. *Biochem. J.* **1991**, *276*, 401−404.

(24) Abbreviations: HL1, 2,6-bis{[*N*-(2-dimethylaminoethyl)-*N*-methyl]aminomethyl}-4-methylphenol; HL2, 2-{[*N*-(2-dimethylaminoethyl)-*N*-methyl]aminomethyl}-4-bromo-6-{[*N*′-2-(2′-pyridyl)ethyl]aminomethyl}-phenolol; cyclen, (1,4,7,10-tetraazacyclododecane; bpta, *N*,*N*-bis(2-pyridylmethyl)-*tert*-butylamine.

Table 1. Summary of X-ray Crystallographic Data

	$[Zn_2L1(\mu\text{-}NO_3)(NO_3)_2]$	$[Zn_2L_1(\mu\text{-}OMe)(NO_3)_2]$	$[Zn_2L_2(NO_3)_3]$	$[Zn_2L_1(\mu\text{-}OH)(NO_3)_2]$
formula	$C_{19}H_{35}N_7O_{10}Zn_2$	$C_{20}H_{38}N_6O_8Zn_2$	$C_{20}H_{28}BrN_7O_{10}Zn_2$	$C_{19}H_{36}N_6O_8Zn_2$
fw	652.28	621.30	737.14	607.28
cryst. system	tetragonal	monoclinic	monoclinic	monoclinic
space group	$P42_1c$	$P2_1/c$	$P2_1/c$	$C2/c$
a, Å	25.0187(3)	10.4432(4)	8.64890(10)	14.017(5)
b, Å		8.7916(4)	17.2821(2)	11.416(5)
c, Å	8.6641(2)	29.4646(12)	19.5061(5)	16.931(5)
β, deg		97.298(1)	97.583(1)	111.462(5)
V, Å^3	5423.17(16)	2683.30(19)	2890.10(9)	2521.4(16)
Z	8	4	4	4
T, K	188(2)	188(2)	188(2)	188(2)
ρ_{calc}, g cm^{-3}	1.598	1.538	1.694	1.600
μ(Mo Kα), mm^{-1}	1.833	1.841	3.104	1.957
2Θ range, deg	3−57	4−57	3−56	5−57
total no. of data	33564	16394	17769	7739
no. of unique data	6443	6257	6646	2930
no. of obsd. data[a]	4653	4193	5790	2131
no. of params	350	333	418	168
R^b	0.0409	0.0433	0.0381	0.0353
wR^2 [c]	0.0772	0.1209	0.1384	0.0942

[a] Observed criterion: $I > 2\ \sigma(I)$. [b] $R = \sum||F_o| - |F_c||/\sum|F_o|$. [c] $wR^2 = \{\sum[w(F_o^2 - F_c^2)^2/\sum[w(F_o^2)^2]\}^{1/2}$.

IR spectra were recorded on a Biorad FTS-135 FTIR spectrometer between 1000 and 3000 cm^{-1} using CaF_2 cells at room temperature.

Ligand Syntheses. Reactions were carried out under an atmosphere of dinitrogen. The ligand HL_1 was synthesized according to a published procedure,[25] as discussed in the Supporting Information. The ligand HL_2 was synthesized by a modification of a published procedure, as described in Scheme S1.[26] The ligand *N*,*N*-bis(2-pyridylmethyl)-*tert*-butylamine (bpta) was synthesized as described previously.[27]

Zinc Complexes. $[Zn_2L_1(\mu\text{-}NO_3)(NO_3)_2]$. The ligand HL_1 (0.035 g, 0.105 mmol) in ethanol (1.5 mL) and $LiOH\cdot H_2O$ (0.004 g, 0.105 mmol) in H_2O (0.2 mL) were mixed and stirred at room temperature for 10 min. A solution of $Zn(NO_3)_2\cdot 6H_2O$ (0.062 g, 0.210 mmol) in ethanol (1.5 mL) was then added. The initially clear reaction mixture turned milky upon stirring, and after 30 min the product $[Zn_2L_1(\mu\text{-}NO_3)(NO_3)_2]$ appeared as a white precipitate. It was filtered off and dried under vacuum. The yield was 0.048 g (70%). ^{1}H NMR in D_2O: δ 6.96 s (2H), 4.25 d (2H), 3.32 d (2H), 2.80 m (8H), 2.50 s (12H), 2.35 s (3H), 2.12 s (6H), for RR and SS isomers; and 6.95 s (2H), 4.00 br (2H), 3.60 br (2H), 2.80 m (8H), 2.50 s (12H), 2.45 s (3H), 2.15 s (6H), for RS and SR isomers. Layering a solution of HL_1 (0.035 g, 0.210 mmol) and $LiOH\cdot H_2O$ (0.004 g, 0.105 mmol) in ethanol (1.5 mL)/H_2O (0.2 mL) with a solution of $Zn(NO_3)_2\cdot 6H_2O$ (0.062 g, 0.105 mmol) in ethanol (1.5 mL) without stirring afforded colorless crystals of $[Zn_2L_1(\mu\text{-}NO_3)(NO_3)_2]$ that were suitable for X-ray analysis. ^{1}H NMR in D_2O: δ 6.96 s (2H), 4.26 d (2H), 3.32 d (2H), 2.80 m (8H), 2.51 s (12H), 2.32 s (3H), 2.15 s (6H), for RR and SS isomers; and 6.95 s (2H), 4.00 br (2H), 3.60 br (2H), 2.80 m (8H), 2.50 s (12H), 2.41 s (3H), 2.15 s (3H), for RS and SR isomers. Calcd for $C_{19}H_{35}N_7O_{10}Zn_2$: C, 34.99; H, 5.41; N, 15.03. Found: C, 34.95, 35.10, 35.05; H, 5.54, 5.58, 5.62; N, 14.57, 14.58, 14.58. The single crystal of $[Zn_2L_1(\mu\text{-}OH)(NO_3)_2]$ identified by X-ray crystallography (vide infra) was obtained as a very minor component by using the same crystallization procedure.

$[Zn_2L_1(\mu\text{-}OMe)(NO_3)_2]$. A procedure similar to that described for preparing $[Zn_2L_1(\mu\text{-}NO_3)(NO_3)_2]$ but using neat methanol as the solvent afforded the methoxide complex $[Zn_2L_1(\mu\text{-}OMe)(NO_3)_2]$ in 65% yield. ^{1}H NMR in DMF-d_7: δ 6.92 s (2H), 4.18 br (2H), 3.62 s (3H), 3.50 br (2H), 2.95 m (4H), 2.50 m (19H), 2.20 s (6H), for RS and SR isomers; and 6.90 s (2H), 4.35 d (2H), 3.60 s (3H), 3.40 d (2H), 2.95 m (4H), 2.60 m (4H), 2.50 m (15H), 2.20 s (6H), for RR and SS isomers. ^{1}H NMR in chloroform-d_1: δ 6.78 s (2H), 4.45 d (2H), 3.50 s (3H), 3.25 d (2H), 2.90 m (4H), 2.30−2.60 m (25H), for RR and SS isomers. ^{1}H NMR in D_2O: δ 6.97 s (2H), 4.25 d (2H), 3.32 d (2H), 2.80 m (8H), 2.51 s (12H), 2.32 s (3H), 2.15 s (6H), for RR and SS isomers; and 6.95 s (2H), 3.98 br (2H), 3.60 br (2H), 2.80 m (8H), 2.50 s (12H), 2.41 s (3H), 2.15 s (3H), for RS and SR isomers; methoxide group is not observed; 3.30 s (free MeOH). Layering solutions of L_1^- and $Zn(NO_3)_2$, as described for $[Zn_2L_1(\mu\text{-}NO_3)(NO_3)_2]$, in neat methanol afforded $[Zn_2L_1(\mu\text{-}OMe)(NO_3)_2]$ as colorless crystals in 50% yield. Calcd for $C_{20}H_{38}N_6O_8Zn_2$: C, 38.66; H, 6.16; N, 13.53. Found: C, 38.44; H, 6.37; N, 13.77.

$[Zn_2L_2(NO_3)_3]$. The ligand HL_2 (0.044 g, 0.104 mmol) in ethanol (2.0 mL) and $LiOH\cdot H_2O$ (0.004 g, 0.105 mmol) in H_2O (0.15 mL) were mixed and stirred at room temperature for 10 min. Then $Zn(NO_3)_2\cdot 6H_2O$ (0.062 g, 0.105 mmol) in ethanol (3.0 mL) was added without stirring. Upon standing at room temperature, the product $[Zn_2L_2(NO_3)_3]$ appeared as light-yellow crystals suitable for X-ray analysis. They were filtered off and dried under vacuum; yield: 0.031 g (40%). Calcd for $C_{20}H_{28}BrN_7O_{10}Zn_2$: C, 32.59; H, 3.83; N, 13.30. Found: C, 32.65; H, 4.07; N, 13.15. ^{1}H NMR in 1:1 D_2O:DMSO-d_6: δ 8.65 br (1H), 8.48 br (1H), 7.91 br d (1H), 7.49 br d (1H), 7.39 t (1H), 7.31 t (1H), 4.18 br (1H), 3.96 br (1H), 3.35 br (1H), 3.20 br (1H), 2.5 br (12H), 2.29 br (6H), 2.27 br (3H).

Mononuclear Complexes. The two mononuclear complexes $[Zn(cyclen)(H_2O)]^{2+}$ and $[Zn(bpta)(H_2O)_2]^{2+}$ were prepared in situ by mixing equivalent amounts of the corresponding ligand and $Zn(OTf)_2$ or $Zn(NO_3)_2\cdot 6H_2O$.

X-ray Crystallography. X-ray crystallographic studies were carried out on a Bruker CCD diffractometer with graphite-monochromatized Mo Kα radiation ($\lambda = 0.71073$ Å) controlled by a pentium-based PC-running the SMART software package.[28] Single crystals were mounted at room temperature on the ends of glass fibers in Paratone N oil, and data were collected at 188 K in a steam of cold dinitrogen maintained by a Bruker LT-2A nitrogen cryostat. Data collection and reduction protocols are described in detail elsewhere.[29] The structures were solved by direct methods and refined using the SHELXTL software package.[30] In general, all non-hydrogen atoms were refined anisotropically. Hydrogen atoms were assigned idealized locations. Empirical absorption corrections were applied to all structures using SADABS.[30] The ethylene and the two methyl groups of the terminal amine nitrogen and the two oxygen atoms of monodentate nitrate in $[Zn_2L_2(NO_3)_3]$ are disordered. The carbon atoms were distributed over the two sets of positions and refined with occupancy factors of 0.71 and 0.29. The two oxygen atoms of the monodentate nitrate were distributed over two sets of positions and refined with occupancy factors of 0.6 and 0.4. Relevant crystallographic information is summarized in Tables 1, 2, and S1−S16 and Figures 1 and S1−S4.

(25) Higuchi, C.; Sakiyama, H.; Okawa, H.; Fenton, D. E. *J. Chem. Soc., Dalton Trans.* **1995**, 4015−4020.

(26) Crane, J. D.; Fenton, D. E.; Latour, J. M.; Smith, A. J. *J. Chem. Soc., Dalton Trans.* **1991**, 2979−2986.

(27) Mok, H. J.; Davis, J. A.; Pal, S.; Mandal, S. K.; Armstrong, W. H. *Inorg. Chim. Acta* **1997**, *263*, 385−394.

(28) *SMART*, version 5.05; Bruker AXS: Madison, WI, 1998.

(29) Feig, A. L.; Bautista, M. T.; Lippard, S. J. *Inorg. Chem.* **1996**, *35*, 6892−6898.

(30) Sheldrick, G. M. *SHELXTL*, V97-2; Siemens Industrial Automation, Inc.: Madison, WI, 1997.

Table 2. Selected Interatomic Distances (Å) and Angles (deg) for the Complexes[a]

complex	bond lengths		bond angles	
$[Zn_2L_1(\mu\text{-}NO_3)(NO_3)_2]$	Zn(1)···Zn(2)	3.2942(6)	Zn(1)−O(1)−Zn(2)	106.5(1)
	Zn(1)−O(1)	2.040(3)	Zn(1)−O(10)−Zn(2)	100.9(1)
	Zn(2)−O(1)	2.070(3)	O(1)−Zn(1)−N(1)	105.8(1)
	Zn(1)−O(4)	2.148(3)	O(1)−Zn(1)−N(2)	94.6(1)
	Zn(2)−O(5)	2.126(3)	O(1)−Zn(1)−O(10)	76.3(1)
	Zn(1)−N(1)	2.121(3)		
	Zn(1)−N(2)	2.125(3)		
$[Zn_2L_1(\mu\text{-}OMe)(NO_3)_2]$	Zn(1)···Zn(2)	3.1093(6)	Zn(1)−O(5)−Zn(2)	104.20(12)
	Zn(1)−O(5)	1.968(3)	Zn(1)−O(1)−Zn(2)	98.16(10)
	Zn(2)−O(5)	1.973(3)	O(1)−Zn(1)−N(1)	102.90(12)
	Zn(1)−O(1)	2.052(2)	O(1)−Zn(1)−N(2)	88.78(11)
	Zn(2)−O(1)	2.063(2)	O(1)−Zn(1)−O(5)	79.01(10)
	Zn(1)−N(1)	2.131(3)		
	Zn(1)−N(2)	2.169(3)		
$[Zn_2L_2(NO_3)_3]$	Zn(1)···Zn(2)	3.394(3)	Zn(1)−O(1)−Zn(2)	117.30(10)
	Zn(1)−N(1)	2.090(3)	O(1)−Zn(1)−N(1)	171.96(10)
	Zn(1)−N(2)	2.059(2)	O(1)−Zn(1)−N(2)	91.20(9)
	Zn(1)−O(1)	2.036(2)	O(1)−Zn(2)−N(6)	132.75(12)
	Zn(2)−N(6)	2.070(3)	O(1)−Zn(2)−N(3)	93.29(10)
	Zn(2)−N(3)	2.132(3)	N(3)−Zn(2)−N(6)	86.83(11)
	Zn(2)−O(1)	1.939(2)		
$[Zn_2L_1(\mu\text{-}OH)(NO_3)_2]$	Zn(1)···Zn(1A)	3.1147(10)	Zn(1)−O(1)−Zn(1A)	105.69(19)
	Zn(1)−O(1)	1.954(3)	Zn(1)−O(5)−Zn(1A)	98.18(12)
	Zn(1)−N(1)	2.145(3)	O(1)−Zn(1)−N(2)	166.62(11)
	Zn(1)−N(2)	2.135(3)	O(1)−Zn(1)−N(1)	103.56(8)
	Zn(1)−O(5)	2.061(2)	O(1)−Zn(1)−O(5)	78.07(12)

[a] Numbers in parentheses are estimated standard deviations of the last significant figure. Atoms are labeled as indicated in Figures 1 and S1−S4.

Potentiometric pH Titrations. All titration experiments were performed on a Brinkmann 176 DMS Titrino instrument equipped with a magnetic stirrer and an automatic pipet. The temperature was measured before and after each experiment and remained constant at a value of 313 ± 0.5 K. The ionic strength of 0.10 M was adjusted with $NaNO_3$. A fresh 0.1 M solution of NaOH calibrated against potassium hydrogen phthalate was used as received to prepare a 0.01 M titrating solution, which was stored in the presence of NaOH pellets in a Brinkmann 176 DMS Titrino instrument and used within 1 or 2 days. Acid deprotonation constants for the aqua ligands were determined by titrating each complex. In a typical experiment, a 1.0×10^{-5} mol portion of a complex was dissolved in 10 mL of aqueous 0.10 M $NaNO_3$. Usually standard 0.0958 N HNO_3 was added to protonate the bridging hydroxide. Then, after 2 min equilibration, a titration experiment was initiated. Experimental data were fit by using the program PKAS to obtain the pK_a values.[31] Titration experiments were repeated three times for each of the complexes, and the reported pK_a values are the averages of these triplicate runs. Potentiometric pH titrations of $HL_1 \cdot 3HBr$ in the presence and absence of $Zn(NO_3)_2 \cdot 6H_2O$ were carried out to determine ligand protonation constants (K_n), zinc(II) complexation constant (K_{Zn_2L}), and deprotonation constants for the zinc(II) complex (K_{Ph}, K_{A1}, K_{A2}). The equilibrium constants are defined in eqs 2−6.

$$H_{n-1}\cdot HL_1 + H^+ = H_n\cdot HL_1 \quad K_n = [H_n\cdot HL_1]/[H_{n-1}\cdot HL_1][H^+] \quad (2)$$

$$HL_1 + 2Zn(II) = Zn_2HL_1 \quad K_{Zn_2L} = [Zn_2HL_1]/[HL_1][Zn(II)]^2 \quad (3)$$

$$Zn_2HL_1 = Zn_2L_1 + H^+ \quad K_{Ph} = [Zn_2L_1][H^+]/[Zn_2HL_1] \quad (4)$$

$$Zn_2L_1(\mu\text{-}H_2O) = Zn_2L_1(\mu\text{-}OH) + H^+$$
$$K_{A1} = [Zn_2L_1(\mu\text{-}OH)][H^+]/[\,Zn_2L_1(\mu\text{-}H_2O)] \quad (5)$$

$$Zn_2L_1(\mu\text{-}OH)(H_2O) = Zn_2L_1(\mu\text{-}OH)(OH) + H^+$$
$$K_{A2} = [Zn_2L_1(\mu\text{-}OH)(H_2O)][H^+]/[Zn_2L_1(\mu\text{-}OH)(OH)] \quad (6)$$

Typically a 1.0×10^{-5} mol portion of $HL_1 \cdot 3HBr$ was dissolved in 10 mL of aqueous 0.10 M $NaNO_3$, followed by optional addition of a 2.0×10^{-5} mol portion of $Zn(NO_3)_2 \cdot 6H_2O$. After 10 min equilibration the titration experiment was started. Experimental data were fit with the program BEST.[31] The value pK_W was 13.54 (at 313 K). Inclusion of equilibria that contain mononuclear zinc(II) species does not affect the fits. Each titration was repeated two times, and the reported values of the equilibrium constants are the averages of these duplicate runs. The deprotonation constants do not change significantly upon addition of 10% DMSO to the aqueous solutions.[32]

Stability of Dinuclear Complexes in Water. The composition of the complexes in aqueous solution was studied by ^{1}H NMR titration experiments at 293 K. The solvent was D_2O for experiments with HL_1, and a 1:1 mixture of D_2O and DMSO-d_6 in experiments with HL_2. The initial concentrations of ligands were determined by comparison with added Ala as an internal standard. The initial concentrations of HL_1 and HL_2, were 0.0640 and 0.0383 M, respectively. In each set of the titration experiments, aliquots of the titrating solutions were added to the NMR tube containing the ligand solution. After each addition, a ^{1}H NMR spectrum was taken. In HL_1 titration experiments, an aliquot of a 1.00 M solution of $Zn(NO_3)_2 \cdot 6H_2O$ in D_2O was added first into the NMR tube, followed by the addition of an aliquot of 1.00 M $LiOH \cdot H_2O$ in D_2O. In HL_2 titration experiments the same composition of the titrating solutions was used but with a 1:1 mixture of D_2O and DMSO-d_6 as the solvent. The concentrations of the ligand and of the complex in the HL_1 titrations were determined from the respective integral areas, with an estimated error of 5−10%. Because the peaks were too broad in the HL_2 titration experiments, owing to exchange, the integration was not performed. Instead, the downfield shift of the ^{1}H resonance at 3.79 ppm was followed for the methylene protons in the pyridine arm after each added aliquot of Zn(II) and base. Dilution of 0.04 M solutions of $[Zn_2L_1(\mu\text{-}NO_3)(NO_3)_2]$ by 10−70-fold did not alter the peak number and positions in the ^{1}H NMR spectra.

Penicillin G Methyl Ester. The ester was synthesized from the sodium salt of penicillin G (5.0 g, 14 mmol) and methyl iodide (1.746 mL, 29.4 mmol) in DMF (60 mL) at room temperature. After 16 h of stirring the solvent was removed under reduced pressure to give a pale yellow oil. This oil was then washed with water (100 mL) and acetone (10 mL). Removal of the solvents followed by drying under vacuum afforded penicillin G methyl ester as a white solid in 50% yield (2.4 g). ^{1}H NMR in $CDCl_3$: δ 7.30 m (5H), 6.25 d (1H), 6.61 dd (1H), 5.47 d (1H), 4.35 s (1H), 3.70 s (3H), 3.60 s (2H), 1.42 s (3H), 1.40 s (3H). ^{13}C NMR in 1:1 D_2O/DMSO δ 174.2 (C(O)N), 170.9 (C(O)N-lactam), 168.5 (COO), 136.4, 129.6, 128.6, 126.9, 70.6, 68.1, 64.5, 59.2, 52.5, 42.0, 30.6, 26.9.

(31) Martell, A. E.; Motekaitis, R. J. *The Determination and Use of Stability Constants*; VCH Publishers: NewYork, 1988.

(32) Bates, R. G.; Paabo, M.; Robinson, R. A. *J. Phys. Chem.* **1963**, *67*, 1833−1838.

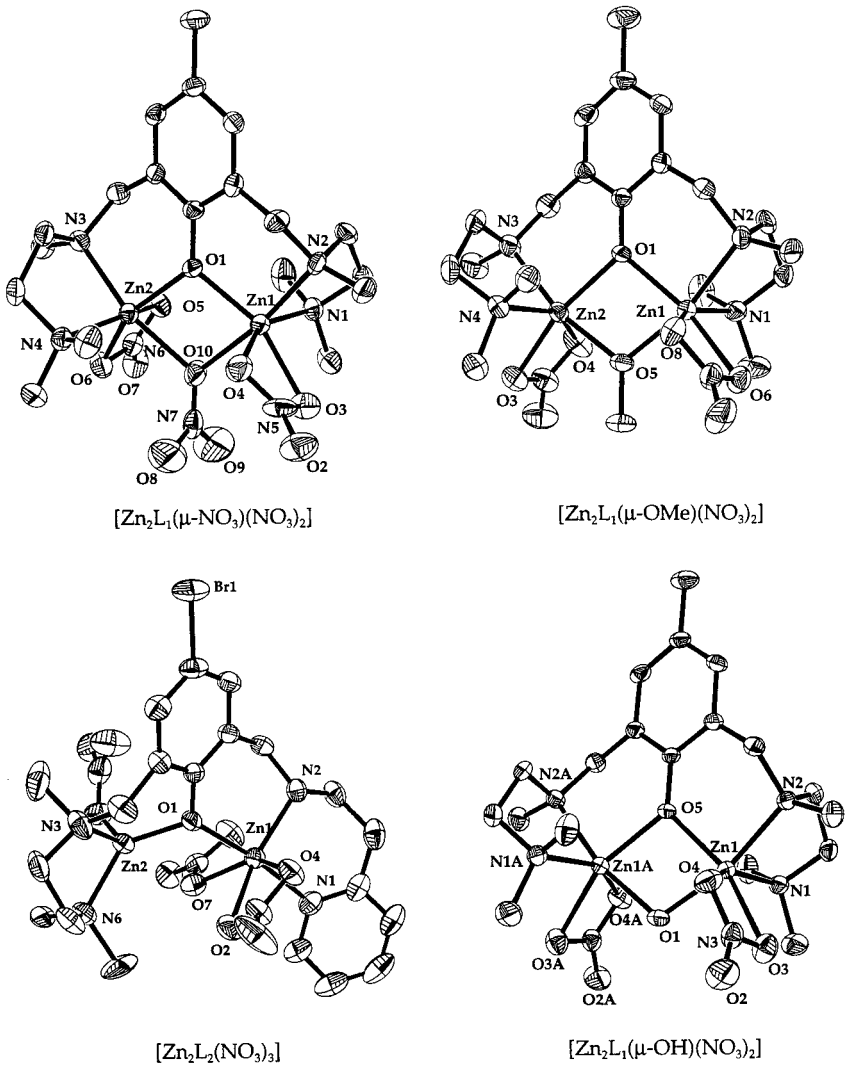

Figure 1. ORTEP diagrams of $[Zn_2L_1(\mu\text{-}NO_3)(NO_3)_2]$, $[Zn_2L_1(\mu\text{-}OMe)(NO_3)_2]$, $[Zn_2L_2(NO_3)_3]$, and $[Zn_2L_1(\mu\text{-}OH)(NO_3)_2]$ showing the 50, 30, 50, and 30% probability thermal ellipsoids for all nonhydrogen atoms, respectively.

Binding of Substrates to Zn(II). *Binding Studies in the Absence of Water.* ^{13}C NMR spectroscopic experiments were carried out, and the chemical shifts are given in ppm relative to DMSO-d_6 as an internal reference. In each experiment, the solution was initially 0.15 M in complex and 0.15 M in penicillin G sodium salt or cephalothin. The solvent was a 1:1 mixture of acetone-d_6:DMSO-d_6 or pure DMSO-d_6 in experiments investigating the binding of penicillin G and DMSO-d_6 for work with cephalothin. The temperature was always 293 K. ^{13}C NMR in 1:1 acetone-d_6/DMSO-d_6 for free penicillin G: δ 174.4 (C(O)N-lactam), 171.7 (COO), 170.6 (C(O)N), 136.4, 129.4, 128.3, 126.6, 74.2, 67.1, 64.5, 57.8, 41.7, 30.8, 27.6. ^{13}C NMR in DMSO-d_6 for free penicillin G (carbonyl region): δ 173.8 (C(O)N-lactam), 170.9 (COO), 170.6 (C(O)N). ^{13}C NMR in 1:1 acetone-d_6/DMSO-d_6 for free cephalothin: δ 174.4 (ester), 173.7 (C(O)N), 167.9 (COO), 165.3 (C(O)N-lactam), 137.4, 133.5, 128.0, 128.5, 126.9, 116.6, 65.6, 60.1, 58.4, 37.4, 26.5, 21.9. ^{13}C NMR in DMSO-d_6 for free cephalothin (carbonyl region): δ 170.6 (ester), 170.0 (C(O)N), 164.3 (COO), 163.1 (C(O)N-lactam). ^{13}C NMR in 1:1 acetone-d_6/DMSO-d_6 for penicillin G in the presence of $[Zn_2L_1(\mu\text{-}NO_3)(NO_3)_2]$ (carbonyl region): δ 174.2 (C(O)N-lactam), 174.1 (COO), 170.8 (C(O)N). ^{13}C NMR in DMSO-d_6 for penicillin G in the presence of Zn(cyclen)$(OTf)_2$ (carbonyl region): δ 173.7 (C(O)N-lactam), 172.3 (COO), 170.6 (C(O)N). ^{13}C NMR in DMSO-d_6 for penicillin G in the presence of Zn(bpta)$(OTf)_2$ (carbonyl region): δ 173.3 (C(O)N-lactam), 172.8 (COO), 170.8 (C(O)N).^{13}C NMR in DMSO-d_6 for cephalothin in the presence of $[Zn_2L_1(\mu\text{-}NO_3)(NO_3)_2]$ (carbonyl region): δ 170.7 (ester), 170.4 (C(O)N), 166.9 (COO), 165.1 (C(O)N-lactam). ^{13}C NMR in DMSO-d_6 for cephalothin in the presence of Zn(cyclen)$(OTf)_2$ (carbonyl region): δ 170.6 (ester), 170.2 (C(O)N), 166.5 (COO), 164.3 (C(O)N-lactam). ^{13}C NMR in DMSO-d_6 for cephalothin in the presence of Zn(bpta)$(OTf)_2$ (carbonyl region): δ 170.4 (ester), 170.2 (C(O)N), 166.9 (COO), 164.1 (C(O)N-lactam).

In a typical solution IR spectroscopic experiment, the initial concentrations of complex and substrate (sodium salt of penicillin G or cephalothin) were 0.05 M each, and the solvent was always DMSO. IR (cm^{-1}) for free penicillin G sodium salt in carbonyl region: 1621 (ν_{asym}(COO)), 1677 (C(O)N), 1767 (C(O)-lactam). Penicillin G in the presence of $[Zn_2L_1(\mu\text{-}NO_3)(NO_3)_2]$: 1638 ($\nu_{asym}$(COO)), 1677 (C(O)N), 1777 (C(O)-lactam). Penicillin G in the presence of Zn(bpta)$(OTf)_2$: 1632 and 1642 (ν_{asym}(COO)), 1677 (C(O)N), 1775 (C(O)-lactam). Free cephalothin: 1617 (ν_{asym}(COO)), 1680 (C(O)N), 1731 (ester), 1773 (C(O)-lactam). Cephalothin in the presence of $[Zn_2L_1(\mu\text{-}NO_3)(NO_3)_2]$: 1630 ($\nu_{asym}$(COO)), 1682 (C(O)N), 1734 (ester), 1777 (C(O)-lactam). IR for penicillin G methyl ester: 1677 (C(O)N), 1750 (C(O)-lactam), 1783 (COOMe).

Binding in Aqueous Solution. The sodium salt of cephalothin (30.0 mg, 0.07 mmol) and the complex $[Zn_2L_1(\mu\text{-}NO_3)(NO_3)_2]$ (45.6 mg, 0.07 mmol) were dissolved in two separate aqueous solutions (1.0 mL each) containing 10% DMSO. Mixing these two solutions resulted in the immediate appearance of a fluffy white precipitate, $[Zn_2L_1(\text{cephalothin})(NO_3)_2]$. The reaction mixture was stirred for an additional 2 h at ambient temperature. The precipitate was filtered, washed with water, and dried in vacuo. ^{13}C NMR in DMSO-d_6 (carbonyl region): δ 170.7 (ester), 170.3 (C(O)N), 166.9 (COO), 165.1 (C(O)N-lactam). Mixing experiments in pure water and in a 1:1 mixture of water and DMSO gave identical results.

Hydrolysis of Penicillin G and Penicillin G Methyl Ester. These reactions were studied by ^{1}H NMR spectroscopy. The solvent was a 1:1 mixture of D_2O and acetone-d_6 and the temperature was 313 K. The initial concentrations of $[Zn_2L_1(\mu\text{-}NO_3)(NO_3)_2]$ and a substrate (penicillin G, sodium salt; and penicillin G, methyl ester) were 0.025 M each. Substrate hydrolysis was followed by monitoring the C(5)−H and C(6)−H resonances at 4.96 and 4.46 ppm in (5*R*)-penicilloic acid, respectively, and at 5.10 and 4.50 ppm in (5*R*)-penicilloic acid-1-methyl ester, respectively.

Kinetics of Hydrolysis. The kinetics of substrate hydrolysis was followed by UV−visible spectrophotometry. The temperature inside the cuvettes was measured directly with a thermocouple. The solvent was either a 9:1 mixture of 0.05 M HEPES buffer and DMSO or a 9:1 mixture of acetone and DMSO. The reported pH values of the solutions correspond to the aqueous component. The substrate used for the kinetic studies was nitrocefin. Its extinction coefficient (ϵ) at 390 nm was determined by measuring the absorbance of solutions containing known concentrations in 9:1 mixtures of 0.05 M HEPES buffer and DMSO at pH values 6.95 and 8.59 and in a 9:1 mixture of acetone and DMSO. The values of ϵ were the same within experimental error in all three media, the average being 21 000 M^{-1} cm^{-1}. Extinction coefficients of the product at 390 and 486 nm were determined in "aged" reaction mixtures and assuming that nitrocefin is completely converted to its hydrolysis product. The values are 7585 M^{-1} cm^{-1} and 16 000 M^{-1} cm^{-1} at 390 and 486 nm, respectively. Stock solutions of the complexes, nitrocefin, and the inhibitor (sodium succinate and sodium acetate) were prepared in the appropriate solvent and used immediately to avoid possible decomposition. The concentrations of stock solutions of complex and nitrocefin were 0.010 M each. The concentrations of the stock solutions of the inhibitors were varied and are specified in each particular experiment. Unless stated otherwise, the concentration of $[Zn_2L_1(\mu\text{-}NO_3)(NO_3)_2]$ in kinetic studies was 5.0×10^{-4} M. In a typical kinetic run all of the reagents were mixed in a spectrophotometric cell and allowed to equilibrate for 2 min inside the temperature-controlled UV−visible spectrophotometer before data collection began. Data were usually collected at 390 nm, the wavelength that corresponds to the maximum absorbance of nitrocefin. Because the reaction product also absorbs at 390 nm ($\epsilon_P = 7585$ M^{-1} cm^{-1}), the extinction coefficient of nitrocefin was corrected, as shown in eqs 7−9 to account for product absorbance.

$$A_T = AS + AP = \epsilon_S c_S + \epsilon_P c_P \tag{7}$$

$$\Delta A_T = \Delta A_S + \Delta A_P = A_S(f) - A_S(i) + A_P(f) - AP(i) = \epsilon_S\{c_S(f) - c_S(i)\} + \epsilon_P c_P(f) = \epsilon_S\{c_S(f) - c_S(i)\} + \epsilon_P\{c_S(i) - c_S(f)\} = \{\epsilon_S - \epsilon_P\}\{c_S(f) - c_S(i)\} \tag{8}$$

$$c_S(f) - c_S(i) = \frac{\Delta A_T}{\epsilon_S - \epsilon_P} \tag{9}$$

In the equations, A_T, A_S, and A_P are the total, substrate, and product absorbances at a given wavelength; ϵ_S and ϵ_P are the extinction coefficients of the substrate and the product at a given wavelength; c_S and c_P are the concentrations of the substrate and the product at a given time; and c(f) and c(i) stand for final and initial concentrations. Data were collected only during the first 3−5% of conversion in each reaction to avoid significant changes in the concentrations of the starting materials. The observed rate constants were then determined from the initial rates, the known concentration of the substrates, and the corrected extinction coefficient of nitrocefin at 390 nm. The rate constants for the formation (k_{form}) and disappearance (k_{dis}) of the anionic intermediate were obtained by fitting the experimental data to eq 10

$$A_t = a\{\exp(-k_{form}t) - \exp(-k_{dis}t)\} \tag{10}$$

where A_t is the absorbance at 640 nm and a is $k_{form}[N]_0/\epsilon(k_{dis} - k_{form})$ ($[N]_0$ − initial concentration of nitrocefin). Nitrocefin and hydrolyzed nitrocefin do not absorb at 640 nm.

Results and Discussion

Preparation of Ligands and Complexes. The dinucleating ligands HL_1 and HL_2 (Scheme 2), derived from 2,4,6-trisubstituted phenol, provide an environment for two zinc(II) ions that resembles those in the active sites of the three metallo-β-lactamases depicted in Scheme 1. Two zinc(II) ions at the active sites are coordinated predominantly by histidine residues[14−16] and are bridged by a hydroxide ion postulated to serve as the nucleophile in hydrolysis. The bridging phenolate and the restricted separation between the two ethylenediamine arms in these ligands strongly favor the formation of dimetallic complexes.[33−35] Although several copper(II) and manganese(II) complexes of ligands in this class, including HL_1, have been synthesized and employed as biomimetic models,[33−36] only a few phenolate-bridged dizinc(II) complexes are known. Included is a dizinc(II) complex having four methoxyethyl chelating arms.[37,38] In the present study, four novel dizinc(II) complexes of HL_1 and HL_2, $[Zn_2L_1(\mu\text{-}NO_3)NO_3)_2]$, $[Zn_2L_1(\mu\text{-}OMe)(NO_3)]$, $[Zn_2L_2(NO_3)_3]$, and $[Zn_2L_1(\mu\text{-}OH)(NO_3)_2]$ were prepared and characterized by X-ray crystallography. The first three were also characterized in solution by ^{1}H NMR spectroscopy.

Structural Studies. The structures of $[Zn_2L_1(\mu\text{-}NO_3)(NO_3)_2]$, $[Zn_2L_1(\mu\text{-}OMe)(NO_3)_2]$, $[Zn_2L_2(NO_3)_3]$, and $[Zn_2L_1(\mu\text{-}OH)(NO_3)_2]$ are presented in Figure 1, and selected bond lengths and angles are provided in Table 2. The complexes $[Zn_2L_1(\mu\text{-}NO_3)(NO_3)_2]$, $[Zn_2L_1(\mu\text{-}OMe)(NO_3)_2]$, and $[Zn_2L_1(\mu\text{-}OH)(NO_3)_2]$ have similar structures. Each zinc(II) ion has a distorted octahedral environment with a bidentate nitrate serving as the terminal ligand. The C_2 symmetry along the phenoxide-4-methyl axis in $[Zn_2L_1(\mu\text{-}OH)(NO_3)_2]$ complex leads to identical coordination spheres of the two zinc atoms. The presence of the two bridging groups in each complex, the phenolate oxygen and either a hydroxide, methoxide, or nitrate ion, results in relatively short Zn···Zn distances of 3.115, 3.109, and 3.294 Å, respectively. The bridging ligand and terminal nitrate ion occupy coordination positions cis to one another. The chirality at N2 and N2A in $[Zn_2L_1(\mu\text{-}OH)(NO_3)_2]$ and at N3 and N2 in $[Zn_2L_1(\mu\text{-}OMe)(NO_3)_2]$ and $[Zn_2L_1(\mu\text{-}NO_3)(NO_3)_2]$ could, in principle, result in the formation of the four diastereoisomers for each complex. The solid-state structures revealed the formation of only RR and SS isomers in each case.

The asymmetric complex $[Zn_2L_2(NO_3)_3]$ contains two zinc(II) ions, Zn1 and Zn2, having distorted octahedral and distorted tetrahedral environments, respectively. The most striking feature of this complex is its lack of an exogenous bridging group; it therefore has a longer Zn···Zn distance compared to the other three compounds, 3.394(3) Å.

Solution Structures. The structures of $[Zn_2L_1(\mu\text{-}NO_3)(NO_3)_2]$ and $[Zn_2L_2(NO_3)_3]$ in solution were investigated by ^{1}H NMR spectroscopy. The resonances of the two methylene groups in HL_1 appear as a singlet for the free ligand. Upon binding to zinc(II), the α and β protons in each methylene group undergo chemical shift changes and become inequivalent. Two pairs of methylene proton resonances occur for $[Zn_2L_1(\mu\text{-}NO_3)(NO_3)_2]$ in aqueous solution, one as well-resolved doublets at 4.25 and 3.32 ppm and the other as broad peaks at 4.00 and 3.60 ppm. We assign the former to the NMR-equivalent RR and SS isomers based upon the following two findings. First, $[Zn_2L_1$-

(33) Sorrell, T. N.; O'Connor, C. J.; Anderson, O. P.; Reibenspies, J. H. *J. Am. Chem. Soc.* **1985**, *107*, 4199−4206.
(34) Mallah, T.; Boillot, M.-L.; Kahn, O.; Gouteron, J.; Jeannin, S.; Jeannin, Y. *Inorg. Chem.* **1986**, *25*, 3058−3065.
(35) Eduok, E. E.; O'Connor, C. J. *Inorg. Chim. Acta* **1984**, *88*, 229−233.
(36) Nasir, M. S.; Cohen, B. I.; Karlin, K. D. *J. Am. Chem. Soc.* **1992**, *114*, 2482−2494.
(37) Uhlenbrock, S.; Krebs, B. *Angew. Chem., Int. Ed. Engl.* **1992**, *31*, 1647−1648.
(38) Sakiyama, H.; Mochizuki, R.; Sugawara, A.; Sakamoto, M.; Nishida, Y.; Yamasaki, M. *J. Chem. Soc., Dalton Trans.* **1999**, 997−1000.

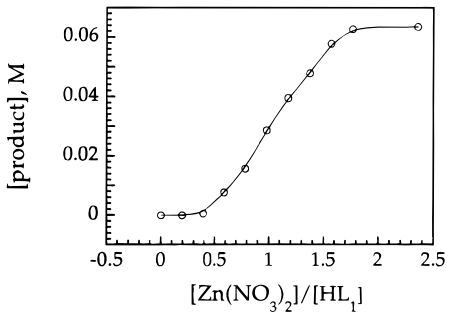

Figure 2. Product formation in titration experiments of HL_1 followed by ^1H NMR spectroscopy. HL_1 was titrated with $Zn(NO_3)_2 \cdot 6H_2O$ and $LiOH \cdot H_2O$.

(μ-NO_3)(NO_3)$_2$], [Zn_2L_1(μ-OH)(NO_3)$_2$], and the analogous methoxide complex [Zn_2L_1(μ-OMe)(NO_3)$_2$] exist as RR and SS isomers in the solid state.[39] Second, the latter complex dissolved in chloroform exhibits α and β proton resonances at chemical

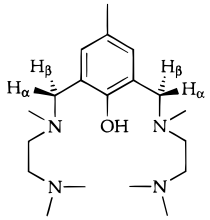

HL_1

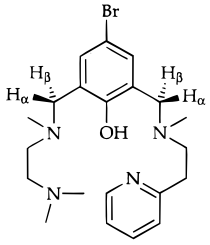

HL_2

shifts of 4.45 and 3.25 ppm that are very similar to the well-resolved resonances of [Zn_2L_1(μ-NO_3)(NO_3)$_2$] in water. The broad pair of resonances is tentatively assigned to NMR-indistinguishable SR and RS isomers. The exchange of the exogenous ligands is not expected to affect the chemical shifts of H_α and H_β.

In ^1H NMR titration experiments, a solution of the ligand was placed in an NMR tube to which the corresponding titrating solution that contained aliquots of $Zn(NO_3)_2 \cdot 6H_2O$ and $LiOH \cdot H_2O$ was added in a stepwise manner, as described in the Experimental Section. The concentrations of the free and bound ligand after each addition were determined by integrating the respective resonances. The experimental titration curve for HL_1 is depicted in Figure 2.

The signals in the ^1H NMR spectrum of [$Zn_2L_2(NO_3)_3$] are rather broad in aqueous DMSO. The H_α and H_β resonances of the methylene groups in HL_2 shift upon coordination, but partial overlap with the HDO resonance and the breadth of the line precluded their accurate integration. Instead, we followed the change upon titration in chemical shift at 3.79 ppm, which corresponds to the pyridine methylene group. The magnitude of this change is directly proportional to the concentration of the complex. The corresponding titration curve is shown in Figure S5.

The concentrations of the bound ligands grow with the stepwise addition of the titrating solution that provides Zn(II) ions and base. Notably, in each case the concentration of the bound ligand is not further altered once the ratio [$Zn(NO_3)_2$]/[ligand] reaches the value of 2. This result indicates that both complexes exist as stable dimetallic species in the presence of water. The sigmoidal curve in Figure 2 is diagnostic of a cooperative interaction between the two Zn(II)-binding sites in HL_1; that is, binding of one Zn(II) ion affects the binding of the second. In this case, the binding of the first Zn(II) ion increases the affinity of HL_1 for the additional Zn(II) ion; the binding is positively cooperative. Ligand HL_2 does not exhibit cooperative binding of Zn(II), as Figure S5 clearly indicates.

Ligand protonation constants (K_n), the zinc(II) complexation constant (K_{Zn_2L}), and deprotonation constants for the zinc(II) complex (K_{Ph}, K_{A1}, K_{A2}) were determined by potentiometric pH titrations of $HL_1 \cdot 3HBr$ in the presence and absence of $Zn(NO_3)_2 \cdot 6H_2O$, as described in the Experimental Section.[40] Typical titration curves for $HL_1 \cdot 3HBr$ are shown in Figure S6A. The mixed protonation constants for the ligand, $\log K_1 - \log K_3$, are 10.09 ± 0.07, 9.40 ± 0.10, and 6.12 ± 0.10, respectively, and agree with literature values.[41−43] The titration curve in the presence of 2 equiv of $Zn(NO_3)_2 \cdot 6H_2O$ reveals the formation of a stable complex at pH > 5.5. Complex formation ($\log K_{Zn_2L} = 13.91 \pm 0.10$) is accompanied by deprotonation of the phenolic group ($pK_{Ph} = 6.97 \pm 0.05$) and an aqua ligand ($pK_{A1} = 7.4 \pm 0.1$). The value pK_{Ph} agrees well with reported constants for the deprotonation of M(II)-bound phenol.[44] Deprotonation of the second aqua ligand ($pK_{A2} = 11.35 \pm 0.12$) requires high pH (>10.0) because the complex already has two anionic ligands.[42] Only dinuclear species were observed under the experimental conditions, as shown in Figure S6B. Therefore, binding of the two zinc(II) ions to HL_1 is nearly simultaneous. Such highly cooperative binding of two zinc(II) ions is known for a binucleating octaazacryptand ligand.[45] Diluting aqueous solutions of [Zn_2L_1(μ-NO_3)(NO_3)$_2$] to 5.0×10^{-4} M does not result in dissociation of zinc(II) because the number and positions of ^1H resonances in the NMR spectra remain the same. This finding supports formation of a stable dinuclear complex in aqueous solution.

Acid Dissociation Constants for the Aqua Ligands. The formation of the coordinated hydroxide at physiological pH is important for efficient metallohydrolase activity because this species often serves as a general base or nucleophile. The complex [Zn_2L_1(μ-NO_3)(NO_3)$_2$] does not contain coordinated water in the solid state (Figure 1). The coordinated nitrates are replaced by aqua ligands upon dissolution in the presence of water. The complex [Zn_2L_1(μ-OH)(NO_3)$_2$], containing bridging hydroxide, was cocrystallized as a minor product together with [Zn_2L_1(μ-NO_3)(NO_3)$_2$]. The pK_a value of 7.40 ± 0.10,[31] determined by titration (Figure S6A), is assigned to the bridging water in [Zn_2L_1(μ-OH_2)$(NO_3)_n$(sol)$_{2-n}$]$^{(2-n)+}$. Terminally bound water would have much higher pK_a value.[43,46] The corresponding dissociation constant for [Zn(cyclen)(H_2O)]$^{2+}$ is 7.9.[41] Bridging water is more acidic than terminally bound water because it interacts simultaneously with two zinc(II) ions. An even greater diminution in pK_a would probably have occurred were it not for the compensating charge of the phenolate bridge in the L_1

(39) Kaminskaia, N. V.; Lippard, S. J. Unpublished results.

(40) The titration curve in the presence of 2 equiv of $Zn(NO_3)_2 \cdot 6H_2O$ reveals the formation of a stable complex at pH > 5.3. The constants $\log K_1$, $\log K_2$, $\log K_{Zn_2L}$, pK_{Ph}, pK_{A1}, and pK_{A2} for $HL_2 \cdot 2HCl$ are 8.55 ± 0.12, 7.03 ± 0.09, 13.78 ± 0.15, 5.89 ± 0.07, 8.28 ± 0.10, and 11.40 ± 0.10, respectively. Therefore under the reaction conditions, at pH = 7.5 and 313 K, less than 3% zinc(II) is free.

(41) Kimura, E.; Nakamura, I.; Koike, T.; Shionoya, M.; Kodama, Y.; Ikeda, T.; Shiro, M. *J. Am. Chem. Soc.* **1994**, *116*, 4764−4771.

(42) Molenveld, P.; Stikvoort, W. M. G.; Kooijman, H.; Spek, A. L.; Engbersen, J. F. J.; Reinhoudt, D. N. *J. Org. Chem.* **1999**, *64*, 3896−3906.

(43) Kimura, E.; Kodama, Y.; Koike, T.; Shiro, M. *J. Am. Chem. Soc.* **1995**, *117*, 8304−8311.

(44) Kimura, E.; Koike, T.; Uenishi, K.; Heidiger, M.; Kuramoto, M.; Joko, S.; Arai, Y.; Kodama, M.; Iitaka, Y. *Inorg. Chem.* **1987**, *26*, 2975−2983.

(45) Koike, T.; Inoue, M.; Kimura, E.; Shiro, M. *J. Am. Chem. Soc.* **1996**, *118*, 3091−3099.

(46) Bazzicalupi, C.; Bencini, A.; Berni, E.; Bianchi, A.; Fedi, V.; Fusi, V.; Giorgi, C.; Paoletti, P.; Valtancoli, B. *Inorg. Chem.* **1999**, *38*, 4115−4122.

Table 3. Reactivities of Various Complexes in the Hydrolysis of Nitrocefin[a]

complex	$10^3 k_{obs}$, min^{-1}
none	<0.07
$[Zn_2L_1(\mu\text{-}NO_3)(NO_3)_2]$	6.0 ± 1.0
$[Zn_2L_1(\mu\text{-}OMe)(NO_3)_2]$	4.2 ± 1.0
$[Zn_2L_2(NO_3)_3]$	13.7 ± 2.0
$Zn(NO_3)_2$	1.3 ± 02
$Zn(cyclen)(NO_3)_2$	2.8 ± 0.3
$Zn(bpta)(NO_3)_2$	7.2 ± 1.1

[a] *T*, 313 K; solvent, 1:9 mixture of DMSO:H_2O at pH 7.50 (adjusted with 0.05 M HEPES buffer); initial concentrations of nitrocefin and a complex = 3.75×10^{-5} and 5.00×10^{-4} M, respectively; concentration of $Zn(NO_3)_2 \cdot 6H_2O = 5.00 \times 10^{-4}$ M.

ligand. The finding that the bridging water in the dinuclear complex can be deprotonated at physiological pH is consistent with its postulated role as the relevant nucleophile in metallohydrolases. The complex $[Zn_2L_2(NO_3)_3]$ has no aqua ligands in the solid state (Figure 1). Upon dissolution in water, one or more nitrate ligands are solvated. The pK_a value of 8.28 ± 0.10 for coordinated water in this complex is tentatively assigned to a terminally bound water molecule.

Effect of Zinc Complexes on Nitrocefin Hydrolysis. Nitrocefin was chosen as the hydrolysis substrate because its hydrolytic reactions (eq 11) can be conveniently followed by

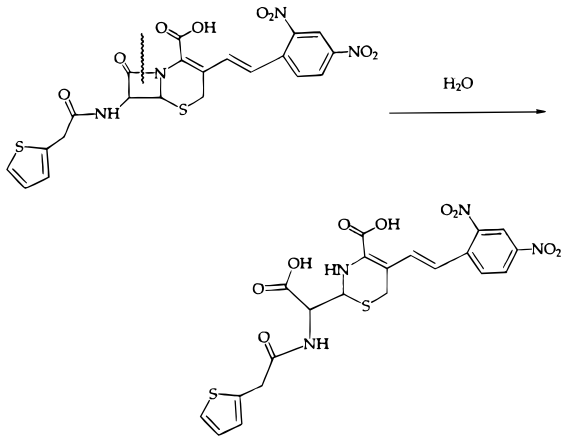

UV−visible spectrophotometry.[47] This compound is one of several related cephalosporins and undergoes a distinctive color change upon hydrolysis by β-lactamases. Nitrocefin absorbs at 390 nm ($\beta = 21\,000$ M^{-1} cm^{-1}). Its absorbance maximum and high extinction coefficient are independent of solvent composition and pH within the range 6.95−8.59. This intense visible absorbance is attributed to the dinitrostyrene substituent on the six-membered ring, resulting in a bathochromic shift due to the conjugation involving the dinitrostyryl group, the β-lactam ring, and the double bond in the dihydrothiazine ring. Upon hydrolysis, the absorbance maximum shifts to 486 nm ($\epsilon = 16\,000$ M^{-1} cm^{-1}), owing to formation of the corresponding cephalosporanoic acid, as shown in eq 11.

All three dizinc complexes catalyze the hydrolysis of nitrocefin in a similar manner, as revealed by the results in Table 3. The dinuclear complexes in Table 3 are 2−10 times more reactive than $Zn(NO_3)_2$. The complex $[Zn_2L_1(\mu\text{-}OMe)(NO_3)_2]$, like $[Zn_2L_1(\mu\text{-}NO_3)(NO_3)_2]$, converts to $[Zn_2L_1(\mu\text{-}OH)(NO_3)_2]$ in aqueous solution, as the ^{1}H NMR data indicate (Experimental Section). Therefore, the reactivities of the first two complexes are similar. Because the two Zn(II) ions at the active sites of

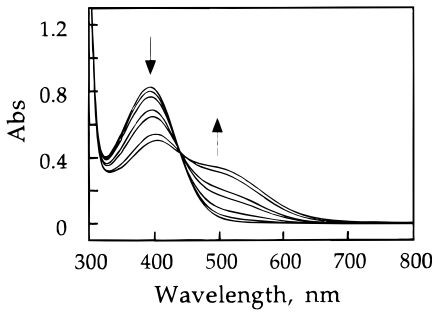

Figure 3. Hydrolysis of nitrocefin in a 1:9 mixture of DMSO:0.05 M HEPES buffer at pH 7.50 followed by UV−visible experiments in the presence of $[Zn_2L_1(\mu\text{-}NO_3)(NO_3)_2]$ at 313 K. Initial concentrations of the complex and nitrocefin were 5.0×10^{-4} and 3.8×10^{-5} M, respectively.

β-lactamases are bridged by a hydroxide ion, the catalytic precursor $[Zn_2L_1(\mu\text{-}NO_3)(NO_3)_2]$ was chosen for further mechanistic studies. As Figure 3 indicates, this complex catalyzes the hydrolysis of nitrocefin without forming any observable intermediates.

Binding of β-Lactam Substrates to Zn(II) Complexes. β-Lactam antibiotics can bind to transition metals via their carboxylate, sulfur atom, β-lactam amide, and terminal amide moieties.[48,49] The mode of binding depends strongly on the metal ion and substrate. It has been suggested that penicillins coordinate via the β-lactam nitrogen atom and the carboxylate group, whereas cephalosporins use the β-lactam oxygen atom for binding.[50,51]

The absorbance maximum and extinction coefficient of nitrocefin are unaffected upon binding to various Zn(II) salts and complexes. ^{1}H NMR spectroscopy is also not very sensitive to β-lactam coordination of metal complexes. The binding and equilibrium constants therefore cannot be deduced on the basis of UV−visible spectrophotometry and ^{1}H NMR experiments. On the other hand, the ^{13}C NMR (160−180 ppm) and infrared (1600−1800 cm^{-1}) spectra of β-lactam carbonyl groups are very sensitive to metal coordination.[52,53] As the data presented here indicate, addition of $[Zn_2L_1(\mu\text{-}NO_3)(NO_3)_2]$ to a solution of penicillin G shifts the ^{13}C resonance of the carboxylate group from 171.7 to 174.2 ppm. The positions of the other resonances do not change significantly. The downfield shift of the carboxylate ^{13}C resonance is characteristic of metal ion coordination.[54] Infrared spectral data reveal that addition of $[Zn_2L_1(\mu\text{-}NO_3)(NO_3)_2]$ to penicillin G in DMSO solution causes 17 and 10 cm^{-1} shifts of the ν_{as}(COO) and ν(C(O)-β-lactam) maxima, respectively. The blue shift and the position of $\nu_{as}(COO^-)$ at 1638 cm^{-1} are consistent with monodentate coordination of the carboxylate group to zinc(II).[55−57] The blue shift in ν(C(O)-β-lactam), moreover, reinforces this assignment by eliminating

(47) O'Callaghan, C. H.; Morris, A.; Kirby, S. M.; Shingler, A. H. *Antimicrob. Agents Chemother.* **1972**, *1*, 283−288.
(48) Grochowski, T.; Samochocka, K. *Polyhedron* **1991**, *10*, 1473−1477.
(49) Asso, M.; Panossian, R.; Guiliano, M. *Spectrosc. Lett.* **1984**, *17*, 271−278.
(50) Gensmantel, N. P.; Gowling, E. W.; Page, M. I. *J. Chem. Soc., Perkin Trans. 2* **1978**, 335−342.
(51) Page, M. I. *Acc. Chem. Res.* **1984**, *17*, 144−151.
(52) Mondelli, R.; Ventura, P. *J. Chem. Soc., Perkin Trans. 2* **1977**, 1749−1752.
(53) Scutaru, D.; Tataru, L.; Mazilu, I.; Diaconu, E.; Lixandru, T.; Simionescu, C. *J. Organomet. Chem.* **1991**, *401*, 81−85.
(54) Kaminskaia, N. V.; Kostic, N. M. *Inorg. Chem.* **1997**, *36*, 5917−5926.
(55) Ferrer, E. G.; Williams, P. A. M. *Polyhedron* **1997**, *16*, 3323−3325.
(56) Zevaco, T. A.; Görls, H.; Dinjus, E. *Polyhedron* **1998**, *17*, 2199−2206.
(57) Kupka, T. *Spectrochim. Acta, Part A* **1997**, *53*, 2649−2658.

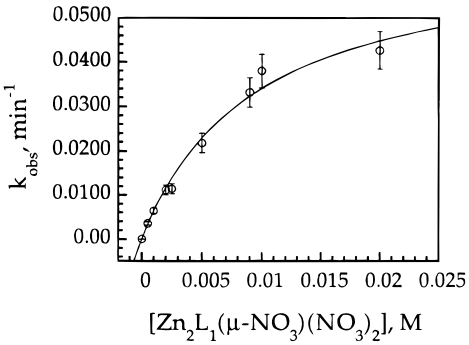

Figure 4. Effect of $[Zn_2L_1(\mu\text{-}NO_3)(NO_3)_2]$ concentration on nitrocefin hydrolysis in at pH = 7.50 in a 1:9 mixture of DMSO and 0.05 M HEPES buffer. Initial concentration of nitrocefin was 3.8×10^{-5} M.

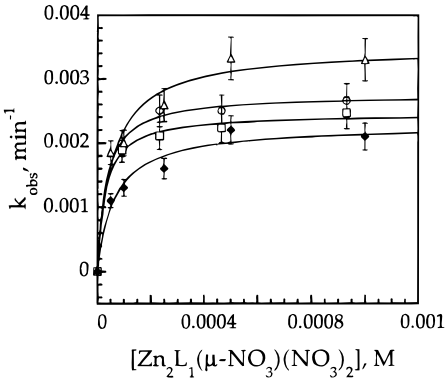

Figure 5. Effect of $[Zn_2L_1(\mu\text{-}NO_3)(NO_3)_2]$ concentration on nitrocefin hydrolysis in a 1:9 mixture of DMSO and acetone in the presence of 0.112 (□), 0.278 (○), 0.556 (◆), and 1.12 (△) M H_2O. Initial concentration of nitrocefin was 3.8×10^{-5} M.

the possibility that coordination occurs via the oxygen atom of this moiety.[57,58] Coordination by the β-lactam nitrogen atom would result in a much higher blue shift than experimentally observed.[59] The small change in ν(C(O)-β-lactam) presumably results from inductive effects originating from zinc binding to the carboxylate group.[57] The mononuclear zinc complexes Zn(bpta)$(OTf)_2$ and Zn(cyclen)$(OTf)_2$ bind to penicillin G only via the carboxylate group, as clearly evidenced by the ^{13}C NMR data in the Experimental Section.

Penicillin G and nitrocefin, which were used in binding and kinetic experiments, respectively, differ somewhat in structure (Scheme S2). We therefore investigated the binding of cephalothin, a nitrocefin-like substrate, by ^{13}C NMR and IR spectroscopy. Addition of $[Zn_2L_1(\mu\text{-}NO_3)(NO_3)_2]$ to a cephalothin solution in DMSO causes a downfield shift of the carboxylic resonance at 163.4 ppm, a clear indication that its carboxylate group binds to zinc(II). The 2-ppm downfield shift of the lactamic carbonyl ^{13}C resonance might suggest coordination by the β-lactam oxygen, but the IR data rule out this possibility. The blue shift and position of $\nu_{as}(COO)$ at 1630 cm^{-1} are consistent with monodentate carboxylate binding to zinc(II). Experiments with Zn(bpta)$(OTf)_2$ and Zn(cyclen)$(OTf)_2$ yield similar results.

Mixing aqueous solutions of $[Zn_2L_1(\mu\text{-}NO_3)(NO_3)_2]$ and cephalothin results in the immediate appearance of a white precipitate $[Zn_2L_1(\text{cephalothin})(NO_3)_2]$ that was isolated. Its ^{13}C NMR spectrum in DMSO-d_6 is identical to that obtained by mixing the complex and cephalothin directly in DMSO solution. Therefore, cephalothin coordinates to $[Zn_2L_1(\mu\text{-}NO_3)(NO_3)_2]$ via the carboxylate group both in aqueous and DMSO solutions.

In summary, penicillin G and cephalothin bind to $[Zn_2L_1(\mu\text{-}NO_3)(NO_3)_2]$ and the mononuclear zinc(II) complexes only by means of a monodentate carboxylate group.

Rate Law for the Hydrolysis of Nitrocefin. Hydrolysis effected by $[Zn_2L_1(\mu\text{-}NO_3)(NO_3)_2]$ follows first-order kinetics with respect to the concentration of nitrocefin, as shown in Figure S7 (Supporting Information). The hydrolysis reaction also increases with $[Zn_2L_1(\mu\text{-}NO_3)(NO_3)_2]$ in a 9:1 mixture of 0.05 M HEPES buffer and DMSO (Figure 4), but this dependence is not linear. This behavior could arise from one of two mechanisms, depicted in Scheme 3, both of which involve coordination of nitrocefin to the dizinc(II) complex. Coordinated nitrocefin is attacked by external water (Scheme 3A) or by zinc(II)-bound hydroxide (Scheme 3B) in bimolecular and unimolecular hydrolyses, respectively. Bimolecular hydrolysis

Scheme 3

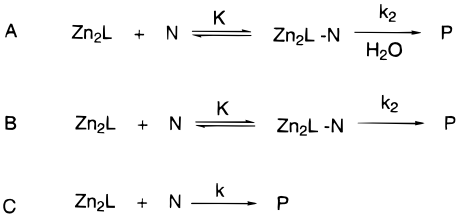

(Scheme 3C), analogous to the hydrolysis of penicillin catalyzed by $[Zn(cyclen)(OH)]^+$ in aqueous solution,[60] can be ruled out because it requires first-order kinetic behavior with respect to the complex. Fitting the experimental data in Figure 4 to eq 12

$$k_{obs} = \frac{Kk_2[Zn_2L]}{K[Zn_2L] + 1} \qquad (12)$$

obtained for Scheme 3B yields a binding constant of 107 ± 20 M^{-1} in a 9:1 mixture of 0.05 M buffer and DMSO at pH 7.50. Water competes with a variety of substrates for binding to transition metal complexes.[54] In the absence of water, the binding of penicillin G and cephalothin to $[Zn_2L_1(\mu\text{-}NO_3)(NO_3)_2]$ is much stronger and can be directly observed by ^{13}C NMR and IR spectroscopy. Therefore, we carried out the hydrolytic reaction in a 1:9 mixture of DMSO and acetone that contained small concentrations of water. As expected, the substrate binds more tightly to $[Zn_2L_1(\mu\text{-}NO_3)(NO_3)_2]$ in this organic solvent, resulting in the saturation kinetics plots depicted in Figure 5. The experimental data were fit to eq 12, derived for Scheme 3B under the condition that $[Zn_2L] \gg [N]$. This fit afforded the binding constant (K) values of $(3.1 \pm 0.5) \times 10^4$, $(2.7 \pm 0.5) \times 10^4$, $(1.5 \pm 0.4) \times 10^4$, and $(1.7 \pm 0.5) \times 10^4$ M^{-1} at 0.112, 0.278, 0.556, and 1.112 M H_2O, respectively.

In conclusion, the kinetic and the binding studies in an organic solvent and aqueous solution rule out the mechanism in Scheme 3C for the hydrolysis of nitrocefin catalyzed by $[Zn_2L_1(\mu\text{-}NO_3)(NO_3)_2]$.

Effect of pH on Hydrolysis Rate. The complex $[Zn_2L_1(\mu\text{-}NO_3)(NO_3)_2]$ hydrolyzes nitrocefin more efficiently at higher pH values, as shown in Figures 6 and S8 (Supporting Information). This finding is consistent with rate-limiting nucleophilic attack of the hydroxo species on the substrate, followed by fast protonation of the intermediate to give the hydrolysis product and regenerated catalyst. The nucleophilicity increases in the

(58) Anacona, J. R.; Figueroa, E. M. *J. Coord. Chem.* **1999**, *48*, 181−189.

(59) Woon, T. C.; Wickramasinghe, W. A.; Fairlie, D. F. *Inorg. Chem.* **1993**, *32*, 2190−2194.

(60) Koike, T.; Takamura, M.; Kimura, E. *J. Am. Chem. Soc.* **1994**, *116*, 8443−8449.

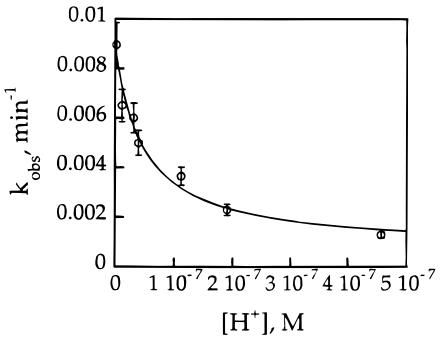

Figure 6. Effect of the solution pH value on nitrocefin hydrolysis catalyzed by $[Zn_2L_1(\mu\text{-}NO_3)(NO_3)_2]$ in a 1:9 mixture of DMSO and 0.05 M HEPES buffer. The rate constants were corrected for the background hydrolysis. Initial concentrations of the complex and nitrocefin were 4.7×10^{-4} and 3.8×10^{-5} M, respectively.

Scheme 4

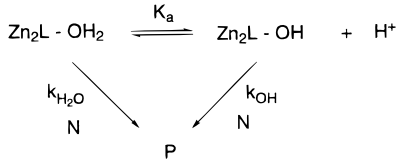

order $Zn_2L\text{-}OH_2 < OH_2 < Zn_2L\text{-}OH < OH^-$. At high pH, the concentration of the more active Zn_2L-OH species is elevated and the hydrolysis is fast.

The experimental results for $[Zn_2L_1(\mu\text{-}NO_3)(NO_3)_2]$ were fit to eq 13, derived for the mechanism in Scheme 4. The fit yielded

$$k_{obs} = \frac{k_{H_2O}[H+] + k_{OH}K_a}{K_a + [H+]} \qquad (13)$$

a pK_a value of 7.5 ± 0.2 for the hydrolytically active species. This value is nearly identical to the pK_a value of 7.40 ± 0.10 for the bridging water in $[Zn_2L_1(\mu\text{-}OH_2)(NO_3)_n(H_2O)_{2-n}]^{(2-n)+}$ obtained by potentiometric titration experiments. Therefore, the bridging hydroxide in this complex acts as the nucleophile in nitrocefin hydrolysis. The respective observed rate constants for the aqua and hydroxo complexes are 1.0×10^{-3} and 1.0×10^{-2} min^{-1}, respectively. The hydroxo complex is only 10 times more reactive than the aqua complex, presumably because the nucleophilicity of μ-OH$^-$ is diminished by binding to two zinc(II) ions simultaneously.

Effect of Water Concentration on the Hydrolysis Rate. The hydrolysis of nitrocefin was investigated at 0.112, 0.278, 0.556, and 1.112 M H_2O as a function of the complex concentration (Figure 5). The respective microscopic rate constants, k_2, $(2.5 \pm 0.4) \times 10^{-3}$, $(2.8 \pm 0.4) \times 10^{-3}$, $(2.3 \pm 0.4) \times 10^{-3}$, and $(3.5 \pm 0.5) \times 10^{-3}$ min^{-1} indicate that hydrolysis of nitrocefin is not affected significantly by changing water concentrations in organic solvent. This finding supports a mechanism in which zinc(II)-bound hydroxide attacks the coordinated substrate (Scheme 3B). The mechanism in Scheme 3A would result in first-order kinetics with respect to $[H_2O]$.[61] Notably, the value of k_2 is ~20-fold lower in an aprotic organic solvent containing small concentrations of water than that in aqueous solution (Figures 4 and 5). This difference might be attributed to the higher pK_a value of μ-OH[62] and decreased stabilizing hydrogen bonding interactions with anionic intermediate in the organic solvent.[63−65] The former factor contributes less than 10-fold to the difference, whereas the latter is responsible for the remaining 2-fold.

Scheme 5

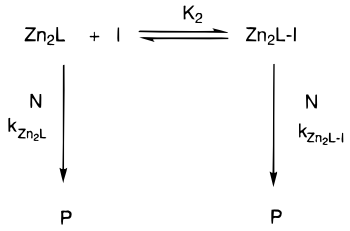

Inhibition. Acetate ion inhibits zinc(II)-catalyzed hydrolysis of nitrocefin (Figure S9A, Supporting Information). The inhibition of $[Zn_2L_1(\mu\text{-}NO_3)(NO_3)_2]$ is best described by the mechanism in Scheme 5 involving formation of the less reactive catalyst upon acetate coordination. Fitting the experimental data in Figure S9 to eq 14 where [I] is the acetate concentration,

$$k_{obs} = \frac{k_{Zn_2L} + k_{Zn_2L-I}K_2[I]}{1 + K_2[I]}[Zn_2L]_0 \qquad (14)$$

yielded a value of 139 ± 46 M^{-1} for K_2. Notably, the apparent binding constant for acetate is nearly identical to that for nitrocefin. This finding corroborates the ^{13}C NMR and IR data on substrate coordination to $[Zn_2L_1(\mu\text{-}NO_3)(NO_3)_2]$. The observed rate constants for the hydrolysis by the catalyst and the inhibited catalyst are $(5.9 \pm 0.2) \times 10^{-3}$ and $(1.1 \pm 0.1) \times 10^{-3}$ min^{-1}, respectively. Sodium succinate is an efficient inhibitor for $[Zn_2L_1(\mu\text{-}NO_3)(NO_3)_2]$, as illustrated in Figure S9B (Supporting Information). Fitting the experimental data to eq 14 yielded values of 1143 ± 260 M^{-1} and $(6.0 \pm 0.1) \times 10^{-3}$ and $(4.5 \pm 0.1) \times 10^{-4}$ min^{-1} for the succinate binding constant and the rate constants for the hydrolysis by catalyst and the inhibited catalyst, respectively. A low-quality X-ray crystal structure reveals that each succinate binds to two Zn(II) ions from different molecules, forming an extended, polymer-like structure. Notably, two succinate molecules actually displace the bridging nitrate or hydroxide that serves as the nucleophile in nitrocefin hydrolysis. Such destruction of the catalyst would explain the low reactivity of $[Zn_2L_1(\mu\text{-}NO_3)(NO_3)_2]$ in the presence of succinate.

Temperature Effects. Because the observed rate constant in aqueous solution is a composite quantity of at least two steps, substrate binding and hydrolysis, the activation parameters obtained from the temperature-dependence plots are also composites. On the other hand, the rate constant in the organic solvent is a microscopic rate constant that corresponds to the hydrolysis of coordinated nitrocefin because nitrocefin is almost entirely bound in the presence of an excess of the catalyst. The zinc(II)-catalyzed hydrolysis of nitrocefin exhibits linear Eyring plot in organic solvent, as shown in Figure 7. A fit of the data to the Eyring equation yielded $\Delta H^{\ddagger}$ and $\Delta S^{\ddagger}$ values of 88.4 ± 5.3 kJ M^{-1} and −45.3 ± 16.0 J M^{-1} K^{-1}, respectively. The enthalpy of activation is higher than those obtained for the hydrolyses of penicillin G promoted by OH$^-$ and the mononuclear complex $[Zn(cyclen)(OH)]^+$.[60] The much less

(61) Raspoet, G.; Nguyen, M. T.; McGarraghy, M.; Hegarty, A. F. *J. Org. Chem.* **1998**, *63*, 6867−6877.

(62) Izutsu, K. *Acid−Base Dissociation Constants in Dipolar Aprotic Solvents*; Blackwell Scientific Publications: Boston, 1990.

(63) Catrina, I. E.; Hengge, A. C. *J. Am. Chem. Soc.* **1999**, *121*, 2156−2163.

(64) The μ-OH complex is a minor species in acetone solution. Therefore, hydrolysis is catalyzed by the aqua complex that is 10 times less reactive than the hydroxide complex.

(65) Reichardt, C. *Solvent Effects in Organic Chemistry*; Verlag Chemie: New York, 1979.

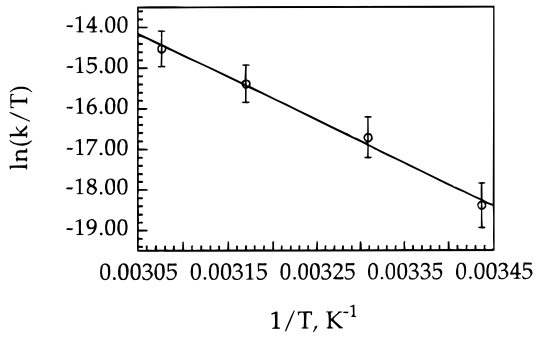

Figure 7. Effect of temperature on nitrocefin hydrolysis catalyzed by $[Zn_2L_1(\mu\text{-}NO_3)(NO_3)_2]$ in a 1:9 mixture of DMSO and acetone. Initial concentrations of the complex, nitrocefin, and water were 9.4×10^{-4}, 3.8×10^{-5}, and 0.278 M, respectively.

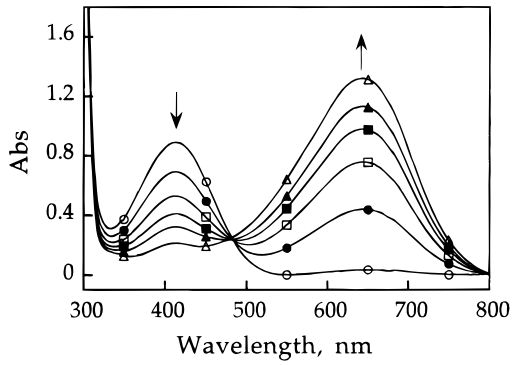

Figure 8. Formation of the intermediate at 640 nm after 1 (○), 10 (●), 20 (□), 30 (■), 40 (▲), and 60 (△) min at 313 K. The solvent was a 1:4 mixture of 0.05 M HEPES buffer (pH = 7.50) and DMSO, the temperature was 313 K. The initial concentrations of $[Zn_2L_1(\mu\text{-}NO_3)(NO_3)_2]$ and nitrocefin were 5.0×10^{-4} and 3.8×10^{-5} M, respectively.

negative $\Delta S^{\ddagger}$ for the hydrolysis by $[Zn_2L_1(\mu\text{-}NO_3)(NO_3)_2]$ supports a mechanism involving intramolecular attack by the bridging hydroxide as the rate-limiting step in nitrocefin hydrolysis.

Role of the Carboxylate. The carboxylate group is "conserved" among β-lactam antibiotics and proposed to orient the substrate at the active site. ^{13}C NMR data reveal that, in simpler model systems, the carboxylate group is always coordinated to zinc(II). Removal of this coordinating anchor by methylation results in significantly decreased rates of hydrolysis of the β-lactam amide bond. Thus, in the presence of $[Zn_2L_1(\mu\text{-}NO_3)(NO_3)_2]$, penicillin G methyl ester is hydrolyzed at least 10^3 times more slowly than penicillin G. Their respective rate constants are 5.1 and <0.007 M^{-1} min^{-1}. A similar effect is observed in reactions catalyzed by $Zn(NO_3)_2$.

Solvent Isotope Effect. Nucleophilic attack of water or hydroxide at the β-lactam carbonyl carbon must be followed by protonation of the amide nitrogen. The relative rates of these two sequential reactions determine the rate-limiting step and, ultimately, the factors that affect the overall reaction. Thus, the increased rate of hydrolysis at high pH and the absence of observable intermediates in aqueous solution are inconsistent with protonation in the rate-limiting step. The effect of solvent isotope composition on hydrolysis was investigated to elucidate further the mechanism. Hydrolytic reactions of nitrocefin in H_2O and D_2O were studied by UV−visible spectrophotometry. Upon dissolution in D_2O, the complex $[Zn_2L_1(\mu\text{-}NO_3)(NO_3)_2]$ will most likely incorporate deuterium into the bridging hydroxide, so the reactivities of Zn_2-OH and Zn_2-OD can be compared. When $[H^+] = [D^+]$ in a reaction mixture (pH = pD = 7.57), the solvent isotope effect, k_H/k_D, was measured to be 0.46. When $[OH^-] = [OD^-]$ (pOH = pOD = 7.4), the solvent isotope effect was 0.204. These results indicate that the Zn(II)-catalyzed hydrolysis of nitrocefin is characterized by a relatively large inverse isotope effect. Free OD^- is 20−40% more reactive as a nucleophile than free OH^-.[66] Presumably Zn(II)-coordinated OD^- is also more reactive than Zn(II)-coordinated OH^-. Our findings are therefore consistent with rate-limiting nucleophilic attack of hydroxide at the substrate, followed by fast protonation.

Formation of the Intermediate. Zinc(II)-catalyzed hydrolysis of nitrocefin in 1:9 mixtures of DMSO and water occurs without the formation of observable intermediates, as shown in Figure 3, presumably because their formation is slower than their disappearance. By contrast, an anionic intermediate (Scheme 1) absorbing at 665 nm was reported for the enzymatic hydrolysis by a metallo-β-lactamase.[20,22] This species is presumably bound to the enzyme via a zinc(II)-acyl linkage and the negatively charged nitrogen-leaving group. It was concluded that electrostatic interaction between the negatively charged intermediate and the positively charged dinuclear zinc(II) center of the enzyme is important for stabilization because addition of exogenous ligands accelerated the collapse of the intermediate.[20] When the water levels in the hydrolysis reaction catalyzed by $[Zn_2L_1(\mu\text{-}NO_3)(NO_3)_2]$ were decreased to 20%, a new species appeared with an absorbance maximum at 640 nm (Figure 8). This species slowly converted to hydrolyzed nitrocefin, as evident from the characteristic absorbance of the latter at 486 nm. This conversion became nearly instantaneous ($t_{1/2} < 0.2$ s) upon addition of acids such as CF_3COOH and CH_3COOH. These findings for the model system are consistent with the formation of an anionic intermediate, similar to that in the enzyme. The small differences in λ_{max} values may be attributed to nitrocefin binding within the hydrophobic enzyme pocket.[22] Hydrophobic environments, like the one in β-lactamase, cause blue shifts of absorbance maxima.[22] Rate constants for intermediate formation and disappearance at 333 K were obtained by fitting the experimental data in Figure S10 to eq 10. Their respective values are 0.25 and 0.006 min^{-1} at 2.78 M H_2O, and 0.09 and 0.03 min^{-1} at 27.8 M H_2O. The formation rate constant is diminished by 2.5-fold at 27.8 M H_2O because water inhibits binding of nitrocefin to the dizinc(II) complex. On the other hand, the disappearance rate constant increased 5-fold at 27.8 M H_2O because water readily displaces the intermediate from the dizinc(II) complex. The free anionic intermediate is unstable and upon protonation converts to hydrolyzed nitrocefin. Increasing water content further diminished the concentration of the intermediate to unobservable levels in aqueous solution.

The Mechanism of the Catalytic Hydrolysis. A mechanism of nitrocefin hydrolysis catalyzed by $[Zn_2L_1(\mu\text{-}NO_3)(NO_3)_2]$ that is consistent with the foregoing results is displayed in Scheme 6. The first step is coordination of the β-lactam carboxylic group to one of the Zn(II) ions. Such binding orients the β-lactam carbonyl carbon and bridging hydroxide in a favorable position for the nucleophilic attack. Although zinc(II) coordination to the β-lactam oxygen was not detected for the substrate, it cannot be ruled out for the transition state. The slightly negative value of $\Delta S^{\ddagger}$ seems to support such a conclusion. In aqueous solution the rate-limiting attack of the bridging hydroxide at the coordinated substrate is followed by fast protonation of the intermediate, then by product release. Slower protonation step in aqueous DMSO results in accumulation of the anionic intermediate. The complex $[Zn_2L_1(\mu\text{-}NO_3)(NO_3)_2]$ is the true

(66) Jencks, W. P. *Catalysis in Chemistry and Enzymology*; Dover Publications, Inc.: New York, 1987.

Scheme 6

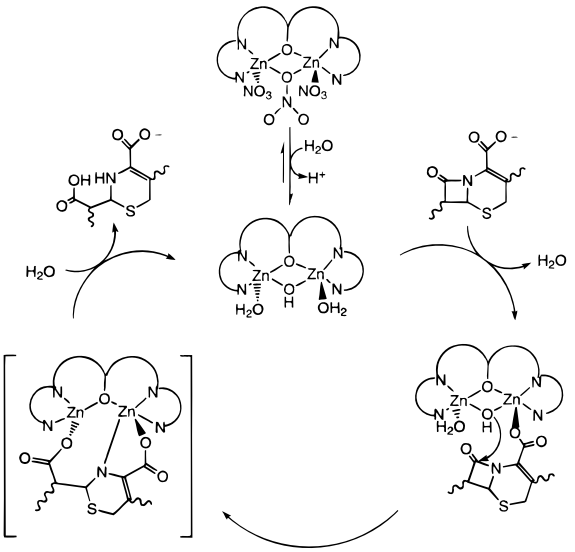

catalyst precursor, because it hydrolyzes at least 10 equiv of nitrocefin, (Figure S11, Supplementary Information). Product inhibition was not detected, presumably because the binding constant is low in aqueous solution.

Nitrocefin Hydrolysis by Mononuclear Complexes. The two mononuclear complexes Zn(cyclen)$(NO_3)_2$ and Zn(bpta)-$(NO_3)_2$ efficiently hydrolyze nitrocefin in aqueous solution, as Table 3 reveals. The aqua ligand in the former complex has a pK_a value of 7.9.[60] The pH dependence for hydrolysis by Zn(bpta)$(NO_3)_2$, shown in Figure S12, yields a pK_a value of 7.84 ± 0.2 for the aqua ligand. These two pK_a values compare well with those of the dinuclear complexes and are sufficiently low for zinc(II)-bound hydroxide to form at physiological pH. The hydrolysis of nitrocefin catalyzed by Zn(bpta)$(NO_3)_2$ follows first-order kinetics with respect to the complex at low concentrations of the complex (Figure S13). Nitrocefin coordination to Zn(bpta)$(NO_3)_2$ causes a leveling off at higher concentrations of complex. Fitting the experimental data to eq 12 yielded values for the binding constants (K) of 1140 ± 106 and 425 ± 90 M^{-1} at 13.9 and 27.8 M H_2O and pH = 7.50. Nitrocefin binds more strongly to Zn(bpta)$(NO_3)_2$ than to $[Zn_2L_1(\mu\text{-}NO_3)(NO_3)_2]$, presumably because zinc(II) is less electrophilic in the dinuclear complex that contains a negatively charged phenolate ligand. The fit also afforded k_2 values of 0.17 and 0.18 min^{-1} at 13.9 and 27.8 M H_2O, respectively. The lack of dependence of hydrolysis of bound nitrocefin on water concentration suggests intramolecular attack by zinc(II)-bound hydroxide. Consequently, the mechanism for Zn(bpta)$(NO_3)_2$ is similar to that for $[Zn_2L_1(\mu\text{-}NO_3)(NO_3)_2]$ and involves initial binding of the substrate, followed by intramolecular hydrolysis by the coordinated hydroxide (Scheme S3). The complex $[Zn(cyclen)(H_2O)]^{2+}$ has fewer coordination sites available for nitrocefin binding and nucleophile activation, and therefore effects hydrolysis in a bimolecular manner according to Scheme 3C.[60,67]

(67) Although β-lactam substrates coordinate to Zn(cyclen)$(OTf)_2$ in organic solvent, this coordination does not take place in water at pH above 7.9. The complex $[Zn(cyclen)(OH)]^+$ is coordinatively saturated. Addition of 1 equiv of Cl^- (an OH^- analog) to an organic solution of $[Zn(cyclen)(penicillin)]^+$ results in complete dissociation of penicillin.

Conclusions and Prospects. We have demonstrated that the bridging hydroxide in the dinuclear zinc(II) complex acts as the nucleophile in hydrolysis of β-lactams and that the carboxylate group of these antibiotics is used for favorable positioning of the substrate and the nucleophile. Therefore, the present model studies support main steps in the suggested mechanism of metallo-β-lactamases.[20] The model complexes, however, lack many active-site residues, such as Asp90, that are available in metallo-β-lactamases. Hence, their activity is inferior to that of the enzymes. Mononuclear Zn(II) complexes are as efficient in nitrocefin hydrolysis as the dinuclear Zn(II) complexes. On the basis of kinetic analyses of various metallo-β-lactamases (Table S17), the effect of the second Zn(II) ion on the hydrolysis rate remains controversial.[18,19,68] The addition of the second Zn(II) ion to the active site results in marginal improvement in β-lactam hydrolysis for some cases or inhibition in others. Although the possibility of a switch in the rate-limiting step for mono- and dizinc(II) metallo-β-lactamases exists,[20] it is also likely that, in the absence of Zn2, active side residues (Cys168, His210, and Asp-90 in *B. cereus* enzyme) favor deprotonation of the terminal aqua ligand bound to Zn1. This conclusion is supported by a crystal structure that reveals hydrogen bonding of Zn1-bound water to Cys168 and Asp90.[17] Moreover mutation of Cys168 to Ala results in a 100-fold decrease in k_{cat}, whereas K_m increases.[19] Similarly, K_m values for monozinc(II) metallo-β-lactamase from *B. fragilis* are lower than those for the dizinc(II) form[18] and C181S mutation results in decreased k_{cat} and increased K_m.[69] Taken together these findings indicate that the role of the second Zn(II) ion in β-lactamases does not involve nucleophile activation.

Acknowledgment. This work was supported under the Merck/MIT Collaboration Program. B.S. thanks the Swiss National Science Foundation and the Novartis Foundation for postdoctoral support. We are grateful to J. Du Bois, C. He, and A. Barrios for helpful discussions.

Supporting Information Available: Experimental methods for ligand synthesis; Figures S1−S4 showing fully labeled ORTEP diagrams for $[Zn_2L_1(\mu\text{-}NO_3)(NO_3)_2]$, $[Zn_2L_1(\mu\text{-}OMe)(NO_3)_2]$, $[Zn_2L_2(NO_3)]_3$, and $[Zn_2L_1(\mu\text{-}OH)(NO_3)_2]$, respectively; Figures S5−S13 showing ^1H NMR titrations for $[Zn_2L_2(NO_3)_3]$, the titration curves and species distribution for $[Zn_2L_1(\mu\text{-}NO_3)(NO_3)_2]$, effects of nitrocefin concentration and pH value of the solution on hydrolysis by $[Zn_2L_1(\mu\text{-}NO_3)(NO_3)_2]$, inhibiting effects of acetate and succinate, formation of the intermediate, catalytic turnover, pH dependence for Zn(bpta)$(NO_3)_2$, concentration dependence for Zn(bpta)$(NO_3)_2$ in aqueous and organic solvents, respectively; Tables S1−S16 showing relevant crystallographic information for $[Zn_2L_1(\mu\text{-}NO_3)(NO_3)_2]$, $[Zn_2L_1(\mu\text{-}OMe)(NO_3)_2]$, $[Zn_2L_2(NO_3)_3]$, and $[Zn_2L_1(\mu\text{-}OH)(NO_3)_2]$, and Table S17 comparing various β-lactamases in their hydrolytic activity (PDF). A crystallographic file in CIF format. This material is available free of charge via the Internet at http://pubs.acs.org.

JA993704L

(68) Bounaga, S.; Laws, A. P.; Galleni, M.; Page, M. I. *Biochem. J.* **1998**, *331*, 703−711.

(69) Yang, Y.; Keeney, D.; Tang, X.; Canfield, N.; Rasmussen, B. A. *J. Biol. Chem.* **1999**, *274*, 15706−15711.